JOURNAL OF SOLID STATE CHEMISTRY 43, 244–250 (1982)

Magnetic Behavior in the Series $La_xY_{1-x}TiO_3$

J. P. GORAL, J. E. GREEDAN, AND D. A. MACLEAN

Department of Chemistry and Institute for Materials Research, McMaster University, Hamilton, Ontario L8S 4M1, Canada

Received December 21, 1981; in final form February 18, 1982

Single-phase products spanning the entire composition range $LaTiO_3$–$YTiO_3$ were prepared. Magnetization–temperature data suggest a transition from negative Ti^{3+}–Ti^{3+} exchange interactions at the La-rich end to positive exchange interactions at the Y-rich end. The magnetic behavior of the intermediate compositions is complex and not well understood. Inverse susceptibility vs temperature data were fitted to a model including both a Curie–Weiss and temperature-independent term. This temperature-independent term scales linearly with La content. The electrical resistivity of single-crystal samples of $La_{0.1}Y_{0.9}TiO_3$ and $La_{0.2}Y_{0.8}TiO_3$ was measured in the range 225–300 K. These data are characteristic of an activated transport mechanism.

Introduction

The isostructural compounds $LaTiO_3$ and $YTiO_3$ show surprisingly different physical properties. Above 130K, $LaTiO_3$ appears to be metallic. The electrical resistivity, ρ, increases with temperature and the magnetic susceptibility, χ, is temperature independent. These facts are consistent with an itinerant model for the Ti^{3+} d^1 electrons. It seems reasonable to attribute at least part of the temperature-independent susceptibility to Pauli paramagnetism. Below 130K, both ρ and χ increase as the temperature drops. It is not clear whether the Ti^{3+} d electrons are localized or itinerant below this temperature. It is possible that $LaTiO_3$ is a semiconductor in this region. The increase in the susceptibility can be interpreted as the onset of magnetic ordering. An extremely small saturation moment of 7×10^{-3} μ_B/Ti^{3+} ion has been reported at 4.2K, as well as a hysteresis in the magnetic moment vs field curve at the same temperature (*1*). This behavior may indicate weak ferromagnetism due to a canted antiferromagnetic structure.

$YTiO_3$ is a semiconductor. Above 29K, the paramagnetic susceptibility obeys the Curie–Weiss law with a Curie constant essentially that of a spin-only, d^1 system. Below 29K, this compound orders ferromagnetically. A saturation moment of $0.84\mu_B/Ti^{3+}$ ion at 4.2K has been reported (*2*). These facts strongly suggest that the Ti^{3+} d electron is localized in $YTiO_3$ over the entire temperature range investigated.

In both these compounds, the only magnetic electron is the $3d^1$ on Ti^{3+}. Since there are no short Ti–Ti contacts in these materials, the exchange pathway between the Ti^{3+} ions includes an intervening oxide ion, making the Ti–O–Ti bond angle an important parameter. Goodenough and Longo have suggested that the Ti^{3+} d^1 electron may undergo a transition from itinerant to localized electron behavior as the angle decreases from 180° (*3*). The Ti–O–Ti angle

0022-4596/82/090244-07$02.00/0

TABLE I

OXIDATIVE WEIGHT GAIN DATA FOR $La_xY_{1-x}TiO_3$

	Weight gain (theoretical)	Weight gain (observed)	$100 \times \left(\frac{\text{wtg(theo)-wtg(obs)}}{\text{wtg(theo)}}\right)$
$La_{0.3}$	4.00	3.86	3.5
$La_{0.4}$	3.91	3.82	2.3
$La_{0.5}$	3.81	3.84	−0.8
$La_{0.6}$	3.72	3.74	−0.5
$La_{0.7}$	3.64	3.64	0
$La_{0.8}$	3.56	3.62	−1.7
$La_{0.9}$	3.48	3.37	3.2
$La_{0.95}$	3.44	3.35	2.6
$LaTiO_3$	3.41	3.28	3.8

may also determine the sign of the magnetic coupling. Magnetic susceptibility data on the $RTiO_3$ series (R = lanthanide^{3+}) indicate that an itinerant–localized type of transition may occur between $CeTiO_3$ (itinerant) and $PrTiO_3$ (localized) (*4*). The Ti–O–Ti angle in $LaTiO_3$ is 157° compared to 142° in $YTiO_3$ (*5*).

Solid solutions of the form $La_xY_{1-x}TiO_3$ (x = 0.3, 0.4, 0.5, 0.6, 0.7, 0.8, 0.9, 0.95, 1.0) were prepared to investigate the change in magnetic properties between the two systems. Reference will be made to studies on the phases (x = 0, 0.1, 0.2) published previously (*6*).

Sample Preparation and Analysis

All compounds were prepared by arc-melting mixtures of the rare earth oxides R_2O_3, and Ti_2O_3. Single crystals of $La_{0.1}Y_{0.9}TiO_3$ and $La_{0.2}Y_{0.8}TiO_3$ used in resistivity studies were grown by the Czochralski technique. Details are given in a following publication.

The Ti^{3+} content was measured by the weight gain of the product upon air oxidation to $R_2Ti_2O_7$ ($2RTi^{(3+)}O_3 + \frac{1}{2}O_2 \rightarrow R_2Ti_2^{(4+)}O_7$) (Table I). As the products tended to be slightly oxidized, a reduced form of titanium sesquioxide ($\sim Ti_2O_{2.98}$) was used in the preparations.

Cell constants were obtained by a least-squares fit of at least 10 powder diffraction peaks corrected with an internal KCl standard (Table II). Peak overlap was especially severe in the La-rich end of the series. A Guinier camera was used to collect data for the phases $La_{0.6}Y_{0.4}TiO_3$–$La_{0.9}Y_{0.1}TiO_3$. All reflections were consistent with single-phase products having the expected orthorhombic cell (*Pbnm*) common to both end members of the series (*5*). A plot of (rare earth radius)^3 vs cell volume shows no discontinuities (Fig. 1).

Magnetic and Resistivity Measurements

Magnetic data were collected on a PAR

TABLE II

CELL CONSTANTS FOR $La_xY_{1-x}TiO_3$

	a	b	c	V
$YTiO_3$	5.340(5)	5.690(4)	7.611(5)	231.2(5)
$La_{0.1}$	5.366(3)	5.677(3)	7.651(5)	233.1(4)
$La_{0.2}$	5.395(3)	5.672(3)	7.684(5)	235.1(4)
$La_{0.3}$	5.429(5)	5.677(6)	7.725(15)	238.1(9)
$La_{0.4}$	5.462(10)	5.671(6)	7.736(7)	239.6(9)
$La_{0.5}$	5.477(10)	5.667(1)	7.769(8)	241.1(7)
$La_{0.6}$	5.517(11)	5.649(11)	7.815(1)	243.6(12)
$La_{0.7}$	5.589(11)	5.626(6)	7.879(15)	247.7(12)
$La_{0.8}$	5.566(11)	5.623(5)	7.930(16)	248.2(12)
$La_{0.9}$	5.593(11)	5.618(6)	7.937(8)	249.4(10)
$La_{0.95}$	5.626(4)	5.620(6)	7.913(14)	250.2(9)
$LaTiO_3$	5.633(10)	5.614(9)	7.940(6)	251.1(9)

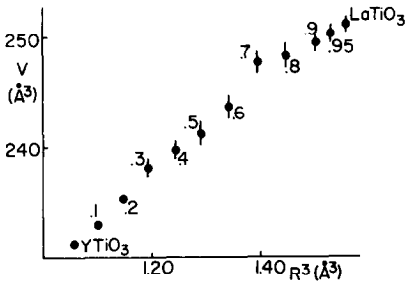

FIG. 1. Cell volume vs (rare earth radius)^3 for $La_xY_{1-x}TiO_3$. The value of x is indicated. The error bars indicate one standard deviation.

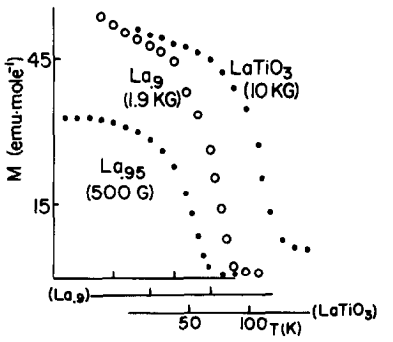

FIG. 3. Magnetization vs temperature for the phases $LaTiO_3$, $La_{0.95}Y_{0.05}TiO_3$, and $La_{0.9}Y_{0.1}TiO_3$. The applied field is given in brackets.

vibrating sample magnetometer using pressed polycrystalline pellets weighing about 500 mg. Magnetization as a function of temperature was investigated for all compounds $La_{0.3}Y_{0.7}TiO_3$–$LaTiO_3$ at applied fields of 0.0045–1.0T. Magnetic moment versus field curves at fields to 1.5T were obtained at various temperatures for the phases $La_{0.3}Y_{0.7}TiO_3$–$La_{0.8}Y_{0.2}TiO_3$ as an aid in locating T_c. Due to the extremely small moment on certain of these compounds, the onset of paramagnetism was determined by the disappearance of hysteresis rather than a zero intercept in the M vs H curve. The uncertainty in the zero of the apparatus is on the order of the observed zero field differences. The magnitude of this remanence increases consistently as the temperature falls below T_c (Fig. 2). Temperature was monitored using a gold–0.07% iron vs chromel thermocouple. Susceptibility data in the range 80–300 K for the compounds $La_xY_{1-x}TiO_3$ (x = 0, 0.1, 0.2, 0.4,

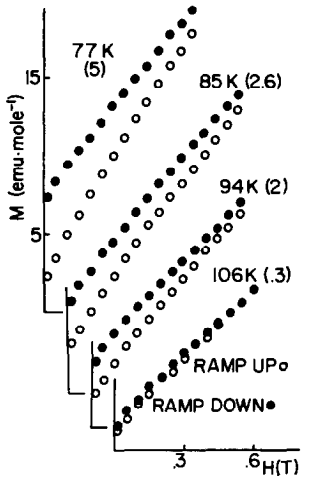

FIG. 2. Magnetic hysteresis measurements for $La_{0.5}Y_{0.5}TiO_3$ at various temperatures. The magnitude of the zero field remanence (emu/mole) is given in brackets.

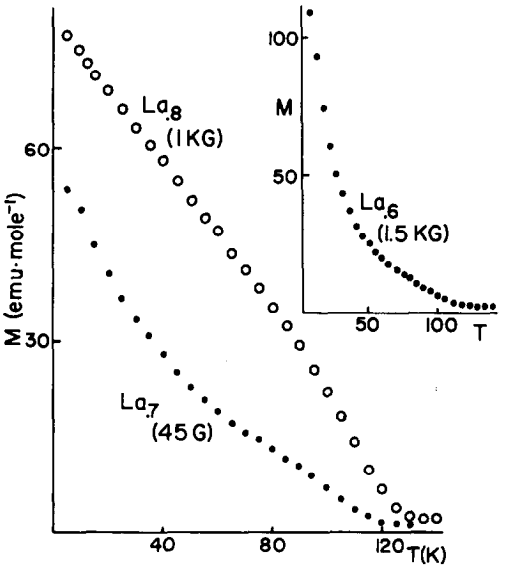

FIG. 4. Magnetization vs temperature for the phases $La_{0.8}Y_{0.2}TiO_3$, $La_{0.7}Y_{0.3}TiO_3$, and $La_{0.6}Y_{0.4}TiO_3$. The applied field is given in brackets.

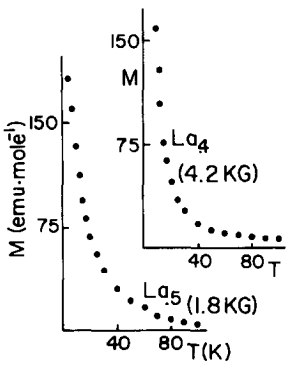

FIG. 5. Magnetization vs temperature for the phases $La_{0.5}Y_{0.5}TiO_3$ and $La_{0.4}Y_{0.6}TiO_3$. The applied field is given in brackets.

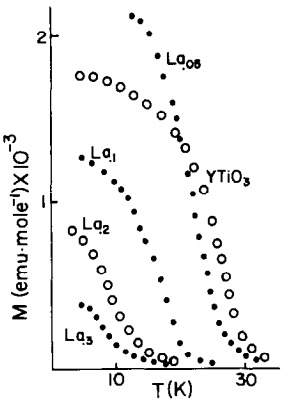

FIG. 6. Low-field magnetization vs temperature for the phases $La_xY_{1-x}TiO_3$ (x = 0, 0.05, 0.1, 0.2, 0.3).

0.7) were obtained using the Faraday technique.

Resistivity data were collected on single-crystal samples of $La_{0.1}Y_{0.9}TiO_3$ and $La_{0.2}Y_{0.8}TiO_3$ in the temperature range 225–300K using the Van der Pauw method (*7*). The crystals were polished into disks of dimensions ~5 × 2 × 0.5 mm.

Results and Discussion

The magnetization–temperature data divide this series into four distinct classes.

(I) For the phases containing 90, 95, and 100% La, a single sharp drop in the magnetization was observed (Fig. 3). T_c can be estimated by a linear extrapolation of M^2 vs T. T_c drops as the Y content increases. The small magnetic moments observed in these compounds point to negative exchange interactions between the titanium ions.

(II) The phases $La_{0.6}Y_{0.4}TiO_3$–$La_{0.8}Y_{0.2}TiO_3$ are characterized by an initial steep drop in the magnetization at low temperature, followed by a region of slightly convex curvature. At higher temperature, the mag-

TABLE III

MAGNETIC DATA FOR $La_xY_{1-x}TiO_3$

	T_c	θ (K)	C^a	$\chi_{TIP}(\times 10^6)$ (cm³ mole⁻¹)	Regression coefficient
$YTiO_3$	29(2)	33[b]	0.35[b]	0[b]	
$La_{0.1}$	19(2)	19	0.27	0	0.9999
$La_{0.2}$	14(2)	1	0.27	180	0.9997
$La_{0.3}$	11(2)				
$La_{0.4}$	43–57	−20	0.17	380	0.9989
$La_{0.5}$	94–106				
$La_{0.6}$	112(4)				
$La_{0.7}$	123(4)	−13	0.04	510	0.9970
$La_{0.8}$	125(4)				
$La_{0.9}$	115(2)				
$La_{0.95}$	127(2)				
$LaTiO_3$	130(2)			800	

[a] In units of cm³ K mole⁻¹.

[b] Data drawn from Ref. (*9*).

netization decreases to a small, nearly constant value (Fig. 4). T_c for these compounds, as determined by the onset of magnetic hysteresis, corresponds to this point at which the magnetization becomes nearly temperature independent. Although within this second group of compounds the critical temperature scales as expected with Y content, it should be noticed that T_c for $La_{0.8}Y_{0.2}TiO_3$ and $La_{0.7}Y_{0.3}TiO_3$ is actually higher than that for the 90% La phase. This may imply the presence of a type of magnetic ordering in these three compounds different than that found in group (I).

(III) $La_{0.5}Y_{0.5}TiO_3$ and $La_{0.6}Y_{0.4}TiO_3$ compose the third group in this series. For both compounds, the magnetization drops sharply and smoothly in the region of 12K (Fig. 5). Surprisingly, hysteresis persists to a much higher temperature. No anomaly was observed in the magnetization–temperature curve in the region where the hysteresis disappears. In the $La_xGd_{1-x}TiO_3$ series, however, anomalies in the magnetization near this temperature region were observed which are greatly suppressed on application of an external magnetic field. An unsuccessful search for hysteresis behavior in $La_{0.3}Y_{0.7}TiO_3$ at higher temperatures confirms that T_c corresponds to the sharp decrease in the magnetization at 11K.

(IV) The remaining phases $La_{0.3}Y_{0.7}TiO_3$–$YTiO_3$ exhibit a single smooth drop in the magnetization (Fig. 6). T_c scales with Y content from a minimum of 11K for the 30% La compound to 29K for $YTiO_3$. The magnitude of the observed magnetic moments implies the presence of positive exchange interactions in these phases.

Thus the magnetic behavior of the intermediate compositions $La_{0.8}Y_{0.2}TiO_3$–$La_{0.4}Y_{0.6}TiO_3$ seems to be much more complex than that of the end members of the series. The values of T_c are summarized in Table III.

The high-temperature inverse susceptibilities of the 10, 20, 40, and 70% La mixtures are shown in Fig. 7. Only that of $La_{0.1}Y_{0.9}TiO_3$ displays the usual linear Curie–Weiss behavior. As the La content increases, the curvature becomes more pronounced. Recalling that the susceptibility of $LaTiO_3$ in this region is temperature independent, the susceptibilities of these phases were expressed in the form

$$\chi_m = C/(T - \theta) + \chi_{TIP}, \qquad (1)$$

where χ_{TIP} represents the temperature-independent contribution. χ of $CeTiO_3$ was analyzed according to this scheme (*1*). Treated in this manner, χ^{-1} for the phases $La_xY_{1-x}TiO_3$ ($x = 0, 0.1, 0.2, 0.4, 0.7$) are presented in Fig. 8. From Table III, it can be seen that the value of the Curie constant, C, drops with La concentration. Paralleling this decrease in C is the near linear increase in χ_{TIP} with La content.

These susceptibility data are consistent with both itinerant and localized electron systems. χ_{TIP} may be interpreted as Van Vleck paramagnetism arising from the effect of the crystal field on the localized Ti^{3+} ion. Previously reported crystallographic data indicate that as the La content increases, the environment of the Ti^{3+} ion be-

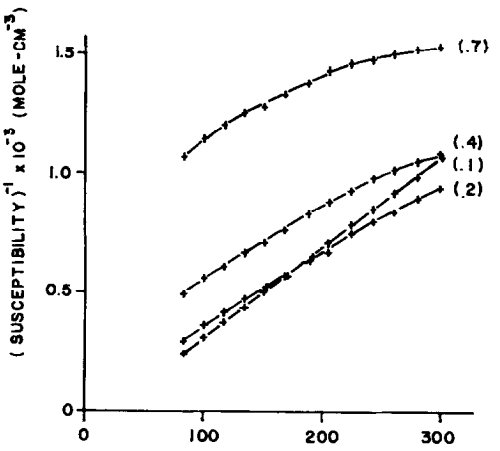

FIG. 7. Inverse susceptibility vs temperature for the phases $La_xY_{1-x}TiO_3$ ($x = 0.1, 0.2, 0.3, 0.4$). The value of x is given in brackets.

comes more ideally cubic (*5*). Thus the nonmagnetic ground state predicted for a $3d^1$ system under the influence of spin–orbit and cubic crystal field perturbations would be more closely realized (*8*). This model predicts the growing predominance of χ_{TIP} as the La content increases and as the Curie constant decreases.

The observed dependence of χ_{TIP} and C on La composition is also consistent with a growth in itinerant character of the Ti^{3+} electrons toward the La-rich end of the series. Since both these models predict similar behavior, the magnetic data alone are insufficient to resolve the ambiguity. From the inverse susceptibility data, it can also be seen that θ becomes smaller as the La content increases, changing sign at the 40% La phase. This may indicate the importance of negative exchange interactions or crystal field effects.

Resistivity data collected on the phases $La_{0.1}Y_{0.9}TiO_3$ and $La_{0.2}Y_{0.8}TiO_3$ in the region 225–300K show a linear increase in ln ρ with T^{-1} (Fig. 9). Recall that $La_{0.2}Y_{0.8}TiO_3$ exhibits a substantial χ_{TIP}. This evidence indicates an activated rather than a metallic transport mechanism. Thus for the Y-rich compounds at least, it seems reasonable to attribute the bulk of χ_{TIP} to Van Vleck paramagnetism arising from crystal field effects rather than to Pauli paramagnetism.

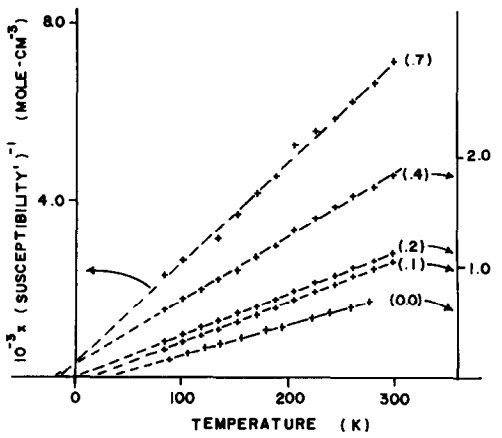

FIG. 8. Inverse susceptibility vs temperature corrected after Eq. (1) for the phases $La_xY_{1-x}TiO_3$ (x = 0, 0.1, 0.2, 0.4, 0.7). The value of x is given in brackets.

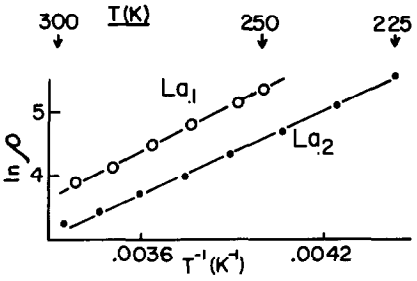

FIG. 9. Natural logarithm of the electrical resistivity (ohm-cm) vs reciprocal temperature for the phases $La_{0.1}Y_{0.9}TiO_3$ and $La_{0.2}Y_{0.8}TiO_3$. The activation energies are 0.221(4) eV · $mole^{-1}$ and 0.187(4) eV · $mole^{-1}$, respectively.

Conclusions

The $La_xY_{1-x}TiO_3$ solid solutions can be divided into four groups based on the temperature dependence of the magnetization.

(I) $LaTiO_3$–$La_{0.9}Y_{0.1}TiO_3$. The magnetization–temperature curves of these compounds are Brillouin-like, consistent with weak ferromagnetism, possibly arising from a canted antiferromagnetic structure.

(II) $La_{0.8}Y_{0.2}TiO_3$–$La_{0.6}Y_{0.4}TiO_3$. These phases are characterized by the unusual curvature of the M vs T plots. T_c corresponds to the appearance of a high-temperature anomaly in the magnetization. This behavior implies a complex magnetic structure.

(III) $La_{0.5}Y_{0.5}TiO_3$–$La_{0.4}Y_{0.6}TiO_3$. Like group (II), these compounds exhibit a critical temperature above 40K, although no associated anomaly is present in the magnetization near T_c.

(IV) $La_{0.3}Y_{0.7}TiO_3$–$YTiO_3$. The magnetization–temperature behavior of these phases points to a well-behaved ferromagnetic system.

High-temperature susceptibility data for the phases $La_xY_{1-x}TiO_3$ (x = 0, 0.1, 0.2, 0.4, 0.7) were successfully fitted to a model

assuming a Curie–Weiss plus a temperature-independent term. The observed dependence of χ_{TIP} and C on La composition is consistent with both an increase in itinerant electron behavior and the evolution of crystal field effects in a localized electron system. Resistivity data collected on $La_{0.1}Y_{0.9}TiO_3$ and $La_{0.2}Y_{0.8}TiO_3$ are inconsistent with metallic electron behavior.

Acknowledgments

We wish to thank Dr. C. V. Stager and Dr. R. Datars for the use of the laboratory equipment employed in the magnetic and resistivity measurements. Invaluable technical assistance was provided by Mr. Gord Hewitson. The Guinier camera used in the X-ray studies was made available through Dr. F. Wicks of the Royal Ontario Museum. The high-temperature susceptibility data were obtained using a Faraday balance courtesy of Dr. A. P. B. Lever of York University. This work was supported by the National Sciences and Engineering Research Council of Canada.

References

1. D. A. MacLean and J. E. Greedan, *Inorg. Chem.* **20,** 1025 (1981).
2. J. D. Garrett, J. E. Greedan, and D. A. MacLean, *Mater. Res. Bull.* **16,** 145 (1981).
3. J. B. Goodenough and J. M. Longo, "Crystallographic and Magnetic Properties of Perovskites and Perovskite-Related Compounds," Landolt-Bornstein Tabellen, New Series III/4a, Springer-Verlag, Berlin (1970).
4. D. A. MacLean, K. Seto, and J. E. Greedan, *J. Solid State Chem.* **40,** 241 (1981).
5. D. A. MacLean, Hok-Nam Ng, and J. E. Greedan, *J. Solid State Chem.* **30,** 35 (1979).
6. J. E. Greedan and D. A. MacLean, *Inst. Phys. Conf. Ser.*, No. 37, 249 (1978).
7. L. J. Van der Pauw, *Philips Res. Rep.* **13,** 1 (1958).
8. E. A. Boudreaux and L. N. Mulay, "Theory and Applications of Molecular Paramagnetism," Wiley, New York (1976).
9. D. Johnston, Ph.D. thesis, University of California, San Diego, 1975.